

Influence of pH, Ionic Strength, and Multidentate Ligand on the Interaction of Cd<sup>II</sup> with Biochars

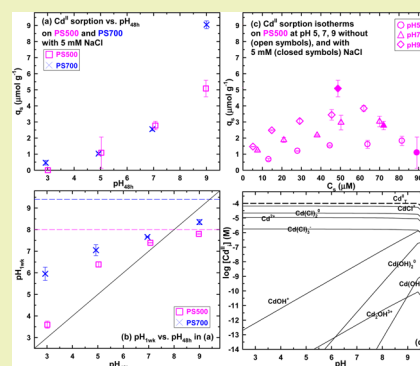
Minori Uchimiya\*

Southern Regional Research Center, Agricultural Research Service, U.S. Department of Agriculture, 1100 Robert E. Lee Boulevard, New Orleans, Louisiana 70124, United States

## Supporting Information

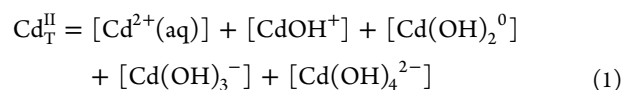
**ABSTRACT:** Pyrolysis temperature-dependent changes in pH, ionic strength, and metal ion-coordinating dissolved organic carbon (DOC) control the sorption of Cd<sup>II</sup> and other transition metals on biochar. Sorption of Cd<sup>II</sup> on 300–700 °C pecan shell biochars was strongly pH- and ionic strength-dependent. Equilibrium speciation calculation suggested that CdOH<sup>+</sup> and other hydrolysis products were the “reactive” Cd<sup>II</sup> species engaging in the surface interaction with biochar. Sorption of Cd<sup>II</sup> on 700 °C (lowest O:C) biochar progressively increased from pH 3 to 7 and was not affected by the citrate concentration. In contrast, low concentration of citrate ([Cd<sup>II</sup>]:[citrate] molar ratios of 4–24) dramatically enhanced Cd<sup>II</sup> sorption on lower temperature (300–500 °C) biochars; higher citrate concentrations diminished Cd<sup>II</sup> sorption. Citrate-enhanced Cd<sup>II</sup> sorption was accompanied by (i) a several-fold increase in DOC and (ii) pH buffering near 7 at equilibrium. Carboxyl ligands form an unusually strong hydrogen bond with the surface functional group of biochar having a similar pK<sub>a</sub>. Sorbed ligand (citrate) could (i) provide new Cd<sup>II</sup> sorption sites on biochar, (ii) buffer pH near 7, and (iii) facilitate the release of higher molecular weight DOC from biochar.

**KEYWORDS:** Chelating agent, Remediation, Activated carbon, Bioenergy, Biomass



## INTRODUCTION

Cadmium(II) and Ni<sup>II</sup> are intrinsically more soluble and less sensitive to surface complexation and precipitation than Pb<sup>II</sup> and Cu<sup>II</sup> in both biochar<sup>1</sup> and soil<sup>2</sup> matrices. Equilibrium dissolved Cd<sup>II</sup> speciation in a noncomplexing electrolyte is dominated by the free aquo species and its hydrolysis products (excluding dimers and tetramers)<sup>3</sup>



Consider the following conditions: 50 μM TOTCd<sup>II</sup> (total dissolved + particulate), I = 0.01 M (NaCl), 25 °C, and Cd(OH)<sub>2</sub>(s,amorphous) as the solubility-limiting phase. At pH 7, soluble species are dominated by Cd<sup>2+</sup> (29.6 μM) and CdCl<sup>+</sup> (19.6 μM), and concentrations of other species are several orders of magnitude lower. The overall rate of Cd<sup>II</sup> sorption on biochar ( $R_{\text{tot}}$ ) can be described as the sum of the rate for each species<sup>4,5</sup>

$$R_{\text{tot}} = \sum_i k_i x_j [i]_s = k_{\text{Cd}^{2+}} x_j [\text{Cd}^{2+}]_s + k_{\text{CdCl}^+} x_j [\text{CdCl}^+]_s + k_{\text{CdCl}_2^0} x_j [\text{CdCl}_2^0]_s + k_{\text{CdCl}_3^-} x_j [\text{CdCl}_3^-]_s + k_{\text{CdOH}^+} x_j [\text{CdOH}^+]_s + k_{\text{CdOH}_2^0} x_j [\text{CdOH}_2^0]_s + k_{\text{CdOH}_3^-} x_j [\text{CdOH}_3^-]_s + k_{\text{CdOH}_4^{2-}} x_j [\text{CdOH}_4^{2-}]_s \quad (2)$$

where  $k_i$  is the rate constant for species  $i$ ,  $[i]_s$  is the surface concentration of species  $i$ , and  $x_j$  is the reactive surface site (e.g., edge functionality, aromatic sheet, ash) of biochar. Before the system reaches equilibrium,  $R_{\text{tot}}$  will control the observable distribution of sorbed ( $q_s$  in mol g<sup>-1</sup> biochar) to dissolved ( $C_s$  in M) Cd<sup>II</sup> species. Intraparticle diffusion (diffusion of sorbed ion along the surface sites of micropore walls) is an example of kinetically slow surface interactions.<sup>6</sup> Some surface sites (e.g., kinks, steps, defect sites) are exceptionally reactive, while other sites are kinetically inert. Similarly, reactive metal species can have a large enough  $k_i$  to contribute to  $R_{\text{tot}}$  even at very low  $[i]_s$ . Metal ion-coordinating dissolved organic carbon (DOC) from biochar and soil will add new Cd<sup>II</sup> species to eq 2. For example, acetate (commonly used pH buffer in biochar experiments) will form three additional species, Cd(acetate)<sup>+</sup>, Cd(acetate)<sub>2</sub><sup>0</sup>, and Cd(acetate)<sub>3</sub><sup>-</sup>, that can interact with the biochar surface differently from the “free” Cd<sup>2+</sup> species. Soluble ligands can also enhance desorption of metal ions from biochar. High stability constants of ethylenediaminetetraacetic acid (EDTA) and related chelating agents are utilized in phytoremediation to lower the toxic metal content of soil.<sup>7</sup> In addition to the solution phase metal–ligand complex formation and competition for surface sites, metal desorption can be

Received: April 2, 2014

Revised: June 30, 2014

Published: July 7, 2014

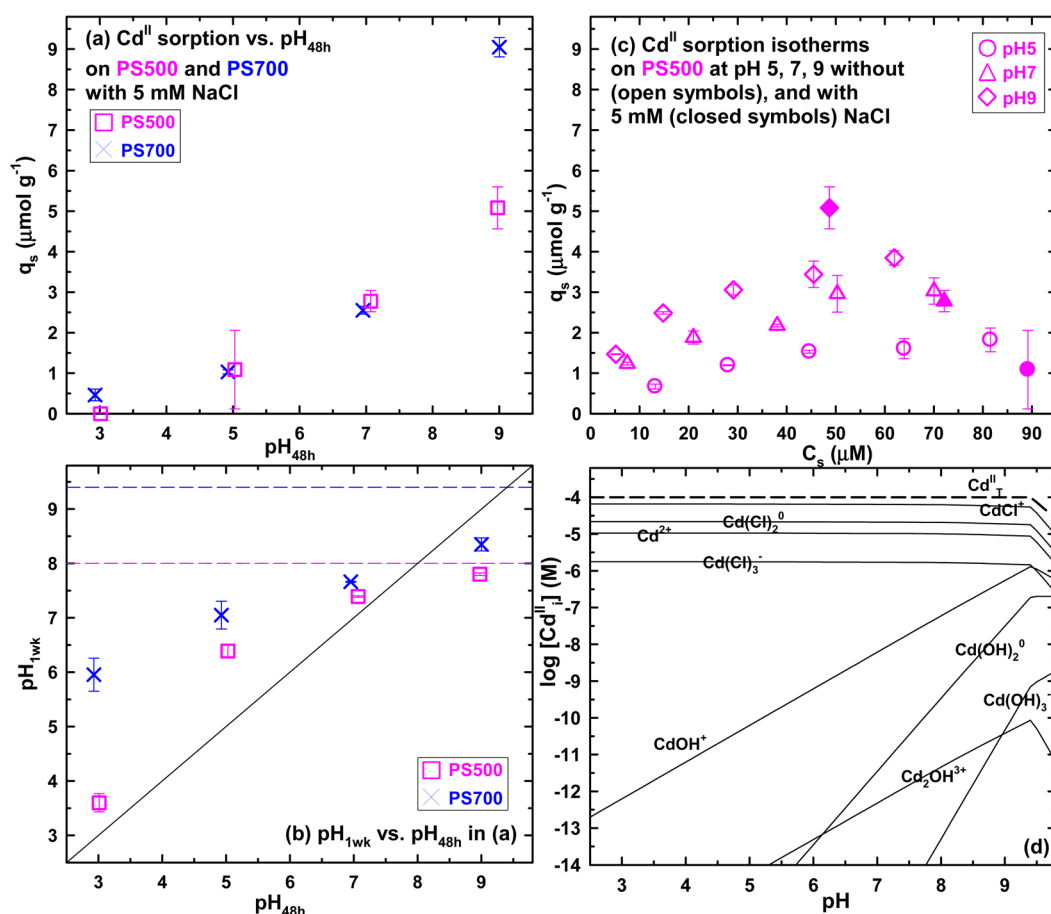


**Figure 1.** (a) Sorbed  $\text{Cd}^{\text{II}}$  ( $q_s$  in  $\mu\text{mol g}^{-1}$  char) and (b) equilibrium pH ( $\text{pH}_{1\text{wk}}$ ) as a function of  $\text{pH}_{48\text{h}}$  (before Cd addition) for pecan shell biochars pyrolyzed at 500 °C (PS500, squares) and 700 °C (PS700, crosses). Horizontal dashed lines in (b) represent native pH of PS500 and PS700; solid line shows the slope of 1. (c)  $\text{Cd}^{\text{II}}$  sorption isotherms on PS500 at  $\text{pH}_{48\text{h}}$  5 ( $\text{pH}_{1\text{wk}} = 7.0 \pm 0.1$ ), 7 ( $\text{pH}_{1\text{wk}} = 7.4 \pm 0.0$ ), and 9 ( $\text{pH}_{1\text{wk}} = 7.6 \pm 0.1$ ). Initial conditions: 100  $\mu\text{M}$   $\text{Cd}^{\text{II}}(\text{NO}_3)_2$ , 5 mM NaCl (a,b and closed symbols in c; no NaCl addition for open symbols in c), and 10  $\text{g L}^{-1}$  biochar. All values are mean  $\pm$  s.d. of duplicate experiments. (d) Cd speciation diagram for 100  $\mu\text{M}$  TOTCd, 10 mM NaCl, and  $\text{Cd}(\text{OH})_2(\text{s,amorphous})$  as the solubility-limiting phase.

induced by acidification and changes in the biochar's surface structure by aging.<sup>8</sup>

As illustrated above, pH, ionic strength, and ligands are the master variables controlling the sorption of  $\text{Cd}^{\text{II}}$  on biochars. Pyrolysis temperature sets these variables in the biochar suspension. Higher pyrolysis temperature typically leads to higher pH and electric conductivity (EC) and lower DOC of biochar.<sup>9</sup> However, these parameters are interdependent of one another. Higher pH induces the release of DOC from biochar, and acidic pH causes ash dissolution to increase EC.<sup>10</sup> In this study, batch sorption experiments were combined with equilibrium speciation calculations to quantitatively predict the  $\text{Cd}^{\text{II}}$  speciation–sorption relationships on pecan shell biochars produced at 300–700 °C.  $\text{Cd}^{\text{II}}$  speciation was systematically altered as a function of pH, ligand concentration, and ionic strength. The biochar property was studied as a function of pyrolysis temperature and by monitoring dissolved organic carbon and phosphorus concentrations at equilibrium. Particular emphasis was given to understand how naturally occurring chelating agent (citrate) will affect the speciation and reactivity of soft Lewis acid  $\text{Cd}^{\text{II}}$ .

## MATERIALS AND METHODS

Distilled deionized water (DDW) with a resistivity of 18  $\text{M}\Omega$  cm (Millipore, Milford, MA) was used for all procedures. Elliott soil humic

acid (ESHA; 1S102H), reference Suwannee River natural organic matter (SRNOM; 1R101N), and standard Suwannee River II humic acid (SRHA; 2S101H) were obtained from International Humic Substance Society (IHSS; St. Paul, MN). All other chemical reagents were obtained from Sigma-Aldrich (Milwaukee, WI) with the highest purity available.

**Biochar Production.** Pecan shells (PS25) were obtained from sheller and were ground (SM 2000 cutting mill, Retsch GmbH, Haan, Germany) and sieved to <2 mm. Pecan shell feedstock was pyrolyzed at 300, 350, 400, 500, 600, and 700 °C under a 1600  $\text{mL min}^{-1}$   $\text{N}_2$  flow rate for 4 h using a laboratory scale box furnace (22 L void volume) with a retort (Lindberg, Type S1662-HR, Watertown, WI). Biochar products were allowed to cool to room temperature overnight under  $\text{N}_2$  atmosphere. Biochars are hereby denoted by the feedstock abbreviation and pyrolysis temperature, e.g., pecan shell feedstock (PS25) and biochars produced at 350 (PS350) and 500 °C (PS500). Detailed procedures for proximate<sup>11</sup> and ultimate analyses and total acidity<sup>12</sup> measurements are provided in Supporting Information.

**$\text{Cd}^{\text{II}}$  Sorption Experiments.** Batch experiments were conducted in duplicate using amber glass vials with Teflon-lined screw caps (40 mL nominal volume, Thermo Fisher Scientific, Waltham, MA) at 10  $\text{g}$  biochar  $\text{L}^{-1}$ ; total volume of each reactor was 30 mL. Biochar suspension was prepared in DDW with and without citric acid or NaCl (to set ionic strength), and the initial pH was recorded as  $\text{pH}_0$  (Orion 3-star plus benchtop pH meter, ThermoScientific, Waltham, MA). For experiments at a fixed pH, 0.1 M HCl or NaOH was used to adjust  $\text{pH}_0$ . Reactors were then pre-equilibrated for 48 h by shaking end-

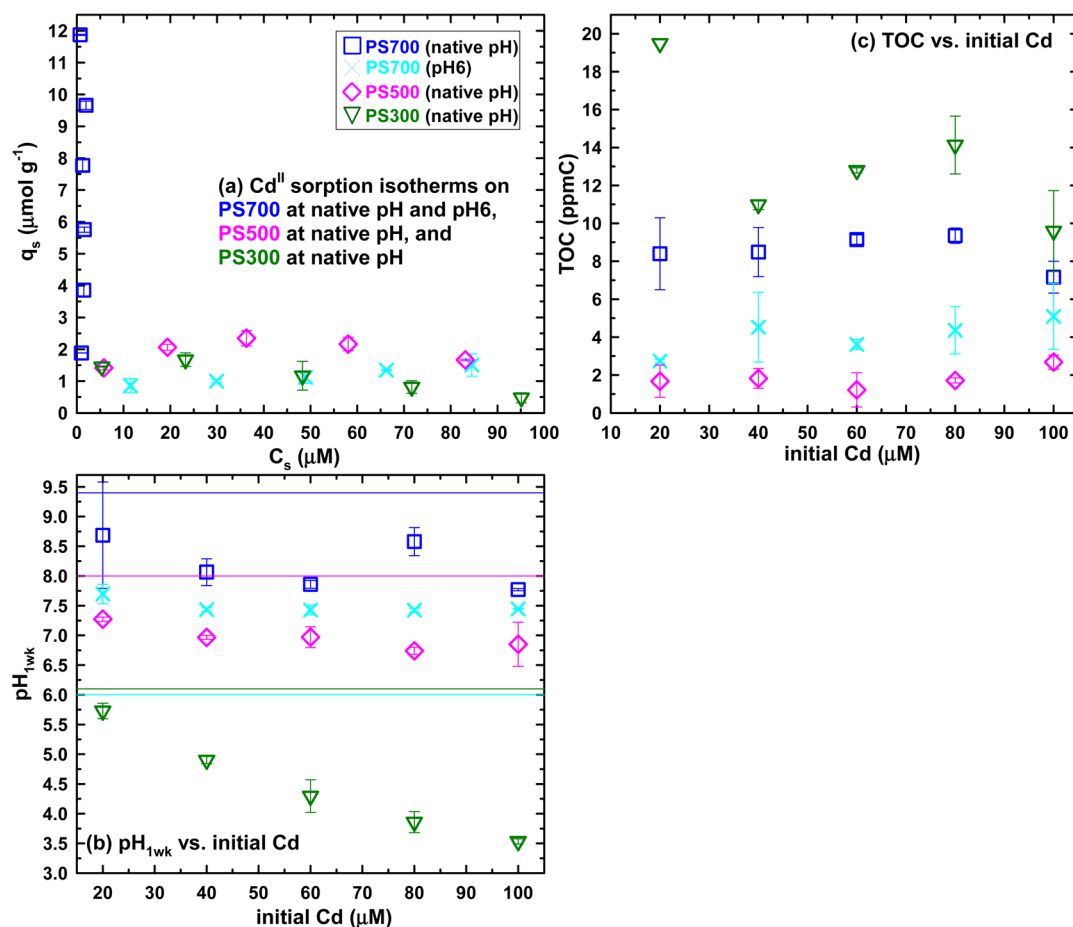


**Figure 2.** (a)  $\text{Cd}^{\text{II}}$  sorption isotherm for PS300, PS500, and PS700 at native pH. Crosses show PS700 at  $\text{pH}_{48\text{h}} = 6$  set by 0.1 M HCl. Equilibrium (b)  $\text{pH}_{1\text{wk}}$  (lines show  $\text{pH}_{48\text{h}}$ ) and (c) TOC as a function of initial Cd concentrations. Initial conditions: 20–100  $\mu\text{M}$   $\text{Cd}^{\text{II}}(\text{NO}_3)_2$ , 10  $\text{g L}^{-1}$  biochar, and no NaCl addition.

over-end at 70 rpm. The pH of each suspension was readjusted using 0.1 M HCl or NaOH for fixed pH experiments and was recorded as  $\text{pH}_{48\text{h}}$ . Subsequently, 9 mM cadmium(II) nitrate tetrahydrate stock solution (prepared daily in 0.1 M HCl) was added to each reactor for the final concentrations of 20–120  $\mu\text{M}$ . Reactors were shaken for 1 wk, and after pH measurement ( $\text{pH}_{1\text{wk}}$ ), they were filtered (0.45  $\mu\text{m}$  Millipore Millex-GS; Millipore, Billerica, MA). Total organic carbon (TOC in ppmC) of filtrate was determined using a Torch combustion TOC/TN analyzer (Teledyne Tekmar, Mason, OH). Soluble Cd, P, Na, and K concentrations were determined after acidifying the filtrate to 4 vol % nitric acid (trace metal grade) using inductively coupled plasma atomic emission spectrometer (ICP-AES; Profile Plus, Teledyne/Leeman Laboratories, Hudson, NH). Blanks, blank spikes, and matrix spikes were included for the quality assurance and control for the ICP-AES analysis.<sup>13</sup>

**Equilibrium  $\text{Cd}^{\text{II}}$  Speciation Calculations.** HYDRAQL<sup>14</sup> equilibrium speciation software was used to calculate the  $\text{Cd}^{\text{II}}$  speciation. Stability constants (Table S1, Supporting Information) at 25  $^{\circ}\text{C}$  were obtained from CRITICAL<sup>3</sup> and were corrected to zero ionic strength using the Davies equation.<sup>10</sup>

## RESULTS AND DISCUSSION

Ultimate (C, H, N, S, and O in wt % on a moisture- and ash-free basis) and proximate (ash, fixed C, moisture, and volatile matter in wt % on a moisture-free basis) analysis results and total acidity of 300–700  $^{\circ}\text{C}$  pecan shell biochars are presented in Table S2 of the Supporting Information. Temperature trends in Table S2 are in agreement with the previous reports.<sup>15,16</sup>

**$\text{Cd}^{\text{II}}$  Sorption at Fixed pH.** Figure 1a presents  $\text{Cd}^{\text{II}}$  sorbed ( $q_s$  in  $\mu\text{mol g}^{-1}$  char) on 500  $^{\circ}\text{C}$  (PS500, squares) and 700  $^{\circ}\text{C}$  (PS700, crosses) pecan shell biochars as a function of  $\text{pH}_{48\text{h}}$ . Initial conditions were 100  $\mu\text{M}$   $\text{Cd}^{\text{II}}$ , 5 mM NaCl, and 10  $\text{g L}^{-1}$  biochar. All values in Figure 1 are given as mean  $\pm$  s.d. of duplicate experiments. The  $\text{pH}_0$  was set using 0.1 M NaOH and HCl. Because the preadjusted  $\text{pH}_0$  of biochar suspensions changed during the 48 h pre-equilibration period, 0.1 M NaOH or HCl was used to readjust pH (to  $\text{pH}_{48\text{h}}$  in Figure 1b) before adding  $\text{Cd}^{\text{II}}$ . Depending on the native pH of the biochar suspension (10  $\text{g L}^{-1}$  suspension in DDW without pH adjustment,  $8.0 \pm 0.1$  for PS500 and  $9.4 \pm 0.0$  for PS700), 0.1–1.7 mM total HCl was necessary to set  $\text{pH}_{48\text{h}}$  in Figure 1a and b. Figure 1a shows a progressive increase in  $q_s$  when  $\text{pH}_{48\text{h}}$  increased from 3, 5, 7, to 9 for both PS500 and PS700. Only for  $\text{pH}_{48\text{h}} = 9$  did PS700 outperform PS500. Similar pH dependence has been observed for  $\text{Cd}^{\text{II}}$  sorption on goethite.<sup>17</sup> Figure 1b shows an increase in pH upon  $\text{Cd}^{\text{II}}$  sorption ( $\text{pH}_{48\text{h}} < \text{pH}_{1\text{wk}}$ ) regardless of  $\text{pH}_{48\text{h}}$  for both PS500 and PS700. The only exception was  $\text{pH}_{48\text{h}} = 9$ ; the solid black line in Figure 1b represents the slope of 1.

Zeta potential measurements of 500 and 700  $^{\circ}\text{C}$  wood biochars showed two inflection points attributable to the dissociation of  $-\text{COOH}$  (pH 6) and  $-\text{OH}$  (pH 10) surface functional groups.<sup>18</sup> When pH of these biochar suspensions (0.5  $\text{g L}^{-1}$ ) was adjusted to 4–10 without buffer, pH increased to 8–10 after 24 h equilibration with and without 2.7  $\text{mg L}^{-1}$

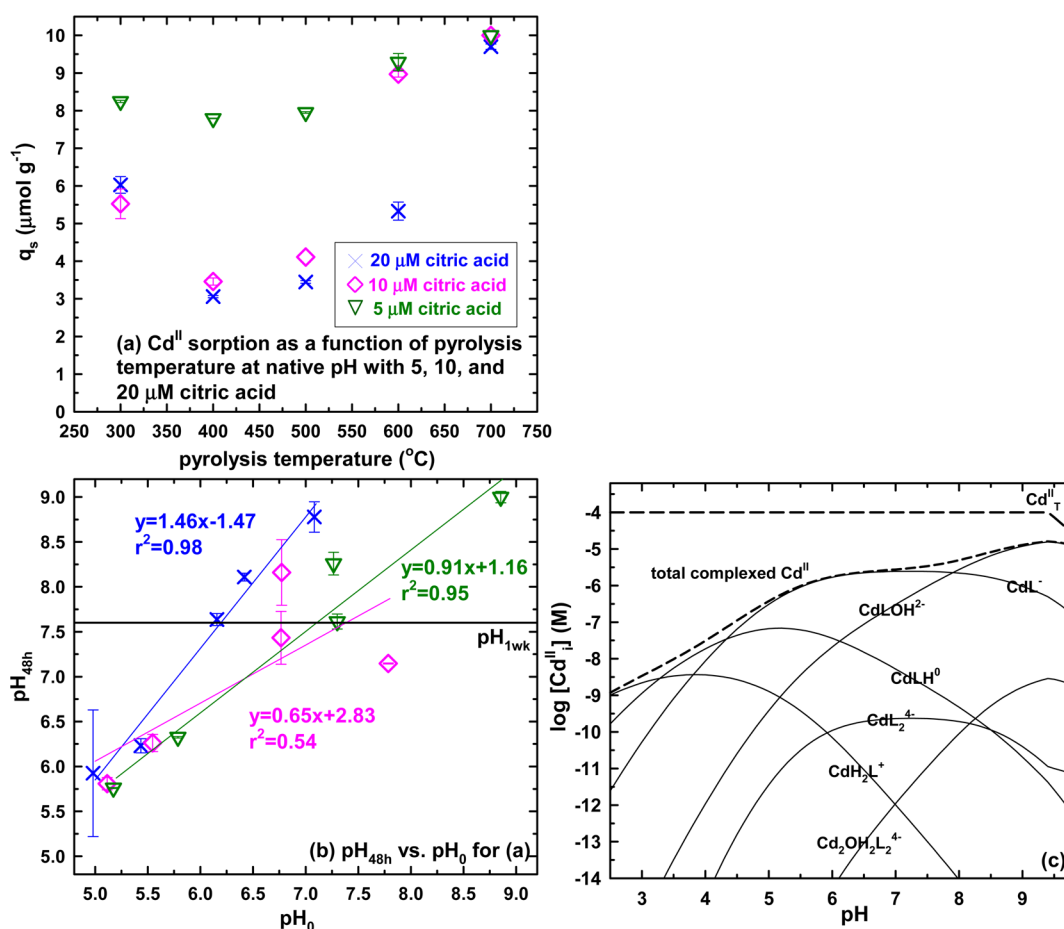


**Figure 3.** (a)  $\text{Cd}^{\text{II}}$  sorption isotherms for PS300, PS400, PS500, PS600, and PS700 in the presence of citric acid. (b)  $\text{pH}_{48\text{h}}$  and  $\text{pH}_0$  corresponding to (a).  $\text{pH}_{1\text{wk}}$  was  $7.6 \pm 0.3$  and is shown as a horizontal black line. Initial conditions:  $100 \mu\text{M Cd}^{\text{II}}(\text{NO}_3)_2$ , 5–20  $\mu\text{M}$  citric acid, and  $10 \text{ g L}^{-1}$  dry biochar without pH adjustment or NaCl addition. (c) Cd–citrate complexes (all other species are given in Figure 1d) in  $100 \mu\text{M TOTCd}$ ,  $20 \mu\text{M}$  citrate,  $10 \text{ mM NaCl}$ , and  $\text{Cd}(\text{OH})_2(\text{s,amorphous})$  as the solubility-limiting phase.

perchlorate.<sup>18</sup> In a separate report, two slow pyrolysis biochars buffered pH at 8.1.<sup>19</sup> Acid–base titration of 500 and 700  $^{\circ}\text{C}$  canola straw biochars showed a plateau at pH 5.5–7.5.<sup>20</sup> The pH range of titration curve plateau (attributable to buffering capacity) coincided with that of the zeta potential measurements.<sup>20</sup> The literature review above indicates that protonation/deprotonation of carboxyl and hydroxyl functionalities contributes to 500–700  $^{\circ}\text{C}$  biochar’s buffering capacity at pH 6–9. Equilibrium pH ( $\text{pH}_{1\text{wk}}$ ) in Figure 1b fell within pH 6–9, except for the lowest  $\text{pH}_{48\text{h}}$  of 3 for PSS00.

Observed pH increase (upon metal sorption, Figure 1b) is the opposite of our previous report on 350 and 700  $^{\circ}\text{C}$  broiler litter biochars.<sup>1</sup> When an order of magnitude greater initial metal concentration (6 mM total; 1.5 mM each of  $\text{Cu}^{\text{II}}$ ,  $\text{Cd}^{\text{II}}$ ,  $\text{Ni}^{\text{II}}$ , and  $\text{Pb}^{\text{II}}$  added together to  $5 \text{ g L}^{-1}$  biochar in 10 mM NaCl) was employed, equilibrium pH was as much as 4 pH units lower than the initial pH.<sup>1</sup> The pH decrease was attributed to the release of exchangeable protons on biochars upon sorption of divalent metal cations.<sup>2</sup> In contrast, a  $<100 \mu\text{M Pb}^{\text{II}}$  addition increased the pH of anaerobically digested manure and sugar beet biochars enriched with dissolved carbonate and phosphate.<sup>21</sup> The pH increase was minimal when sufficiently high  $\text{Pb}^{\text{II}}$  (1–3 mM) was present to form Pb carbonate phases.<sup>21</sup> For  $\text{Cd}^{\text{II}}$ ,  $\text{Cd}_3(\text{PO}_4)_2$  precipitate was observed on manure biochar but not plant biochar.<sup>22</sup>  $\text{Cd}^{\text{II}}$

sorption on plant biochar was hypothesized to occur through surface complexation involving phenolic  $-\text{OH}$ .<sup>21</sup>

In order to understand the pH effects in Figure 1a, Figure 1d presents the concentrations of individual and total ( $\text{Cd}^{\text{II}}_{\text{T}}$ ) soluble  $\text{Cd}^{\text{II}}$  species as a function of pH. Figure 1d was constructed for  $100 \mu\text{M TOTCd}$  (total dissolved + particulate),  $10 \text{ mM NaCl}$ , and  $\text{Cd}(\text{OH})_2(\text{s,amorphous})$  as the solubility-limiting phase. The pH trends in Figure 1a and d suggest that  $\text{Cd}^{\text{II}}$  hydrolysis products are the reactive species (eq 2) on the biochar surface. Point of zero charge (PZC) of  $\geq 500 \text{ }^{\circ}\text{C}$  biochars is expected to be pH 4 or below.<sup>18</sup> Electrostatic interactions will become favorable above pH 4 between the negatively charged biochar surface and positively charged “reactive”  $\text{CdOH}^+$  species in Figure 1d. Additional factors must be considered for the higher reactivity of PS700 than PS500 at pH 9, despite comparable  $\text{pH}_{48\text{h}}$  and  $\text{pH}_{1\text{wk}}$  of the two biochars.

**$\text{Cd}^{\text{II}}$  Sorption at Fixed Ionic Strength.** In order to investigate the influence of ionic strength,  $\text{Cd}^{\text{II}}$  sorption isotherms were obtained on PS500 with 0, 5, and 100 mM NaCl at  $\text{pH}_{48\text{h}} = 5, 7, \text{ and } 9$  (Figure 1c). Without added NaCl (open symbols in Figure 1c), the sum of equilibrium Na and K (primary electrolytes originating from biochar)<sup>23</sup> concentrations was 0.3–0.6 mM and was over 2 orders of magnitude lower than the 100 mM NaCl addition. Without added NaCl,  $\text{Cd}^{\text{II}}$  sorption progressively increased as a function of  $\text{pH}_{48\text{h}}$  (Figure 1c). No  $\text{Cd}^{\text{II}}$  sorption was observed in the presence of

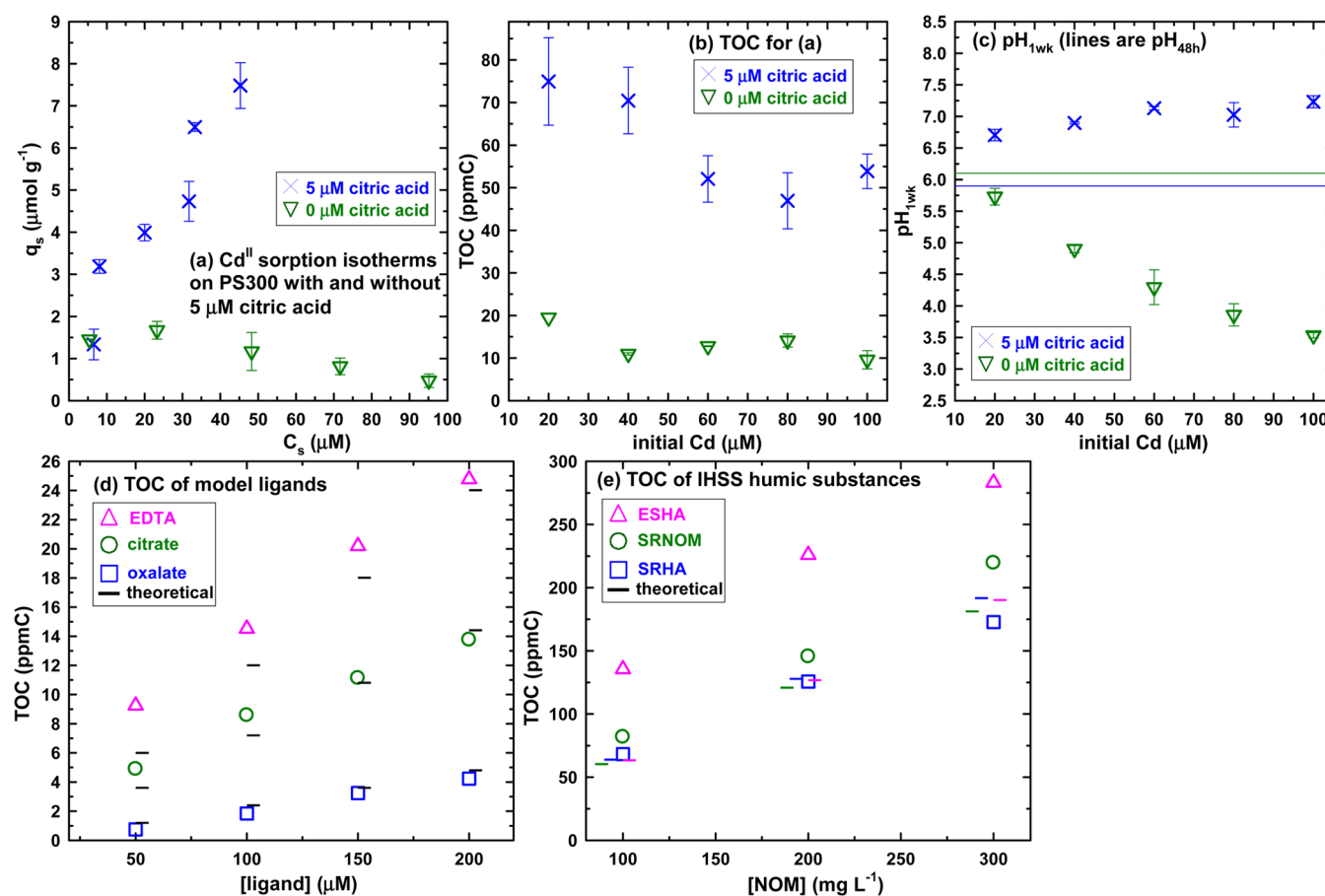


**Figure 4.** Cd<sup>II</sup> sorption isotherms (a), equilibrium TOC (b), and pH (c) for PS300 with 0 and 5 μM citric acid. Initial conditions: 20–120 μM Cd<sup>II</sup>(NO<sub>3</sub>)<sub>2</sub>, 0–5 μM citric acid, and 10 g L<sup>-1</sup> dry biochar without pH adjustment or NaCl addition. Determined (symbols) and theoretical (horizontal line) TOC of model ligands (d) and humic substances (e). Theoretical values in (e) were corrected to account for moisture and ash.

100 mM NaCl. Lower added NaCl concentration (5 mM; closed symbols in Figure 1c) minimally impacted the Cd<sup>II</sup> sorption on PS500 at pH 5, 7, and 9. All subsequent experiments were conducted without NaCl addition.

Ionic strength (I) dependence is traditionally used to differentiate inner-sphere (I independent) and outer-sphere (I dependent) sorption mechanisms.<sup>17</sup> In the outer-sphere mechanism, at least one water molecule remains between the surface functional group and sorbed ion.<sup>10</sup> Classical I effects arise from the competition with supporting electrolyte (Ca<sup>2+</sup>, Na<sup>+</sup>) to form outer-sphere surface complexes.<sup>17</sup> For example, Ca decreased Cd<sup>II</sup> sorption on amorphous ferric hydroxide by >20%, even though the Cd<sup>II</sup> sorption was insensitive to 5–500 mM I set by NaNO<sub>3</sub>.<sup>24</sup> Additional sources of I dependence are charge screening,<sup>25</sup> ion pairs,<sup>17</sup> and changes in the surface activity of solute.<sup>10</sup>

**Cd<sup>II</sup> Sorption without pH Adjustment.** Figure 2a shows Cd<sup>II</sup> sorption isotherms on PS300, PS500, and PS700 without pH adjustment (native pH of biochar suspension). The pH<sub>0</sub> of biochar suspension increased as a function of pyrolysis temperature: 6.1 ± 0.1 for PS300, 8.0 ± 0.1 for PS500, and 9.4 ± 0.0 for PS700. The pH<sub>0</sub> remained constant after 48h pre-equilibration (pH<sub>0</sub> = pH<sub>48h</sub>, lines in Figure 2b) in DDW prior to Cd<sup>II</sup> addition. Compared to PS700 at native pH (squares in Figure 2a), Cd<sup>II</sup> sorption on PS300 and PS500 were negligibly low. However, when pH of the PS700 suspension was adjusted to 6 (crosses in Figure 2a), Cd<sup>II</sup> sorption decreased to the degree of PS300 and PS500 (at native pH). Equilibrium pH

(pH<sub>1wk</sub>, symbols in Figure 2b) was 7.5 ± 0.1 for the PS700 isotherm preadjusted to pH 6 and 8.1 ± 0.5 for native pH. Therefore, the pH dependence for PS700 does not arise from the Cd<sup>II</sup> solubility with respect to hydrolysis (see Cd<sup>II</sup><sub>T</sub> in Figure 1d). Instead, the difference likely originated from (i) Cd<sup>II</sup> speciation at pH<sub>48h</sub> or (ii) surface modification by pH adjustment to 6. Ash content of PS700 was 4.47 ± 0.05 wt % (Table S2, Supporting Information). The pH decrease from 9.4 to 6.0 can cause dissolution of alkali and alkaline earth metals<sup>26</sup> and change the surface property of PS700. Despite a nearly 2 pH unit difference, Cd<sup>II</sup> sorption on PS300 and PS500 were similarly low.

Figure 2b indicates the following trend: pH<sub>1wk</sub> < pH<sub>48h</sub> for PS300, PS500, and PS700 at native pH; pH<sub>1wk</sub> > pH<sub>48h</sub> for PS700 set to pH<sub>48h</sub> = 6. Progressive pH decrease as a function of Cd<sup>II</sup> concentration is visible in Figure 2b for PS300 having the lowest pH<sub>1wk</sub> and pH<sub>48h</sub>. Because Cd<sup>II</sup> sorption by PS300 was low (Figure 2a), the observed pH decrease indicates poor buffering ability of PS300 for Cd<sup>II</sup> and proton from 9 mM Cd(NO<sub>3</sub>)<sub>2</sub> stock solution in 0.1 M HCl. In order to test this, pH was measured immediately after adding Cd<sup>II</sup> for the native pH experiments for PS300 and PS500 in Figure 2 (Figure S1, Supporting Information). Even though pH of both PS300 and PS500 decreased immediately after the Cd<sup>II</sup> addition (Figure S1b, Supporting Information), pH of PS500 reached a nearly constant value (near 7) after 1 wk equilibration (PS500 sorbed more Cd<sup>II</sup> than PS300, Figure 2a). Higher temperature biochar is expected to have a greater pH buffering capacity.<sup>20</sup> Figure 2c

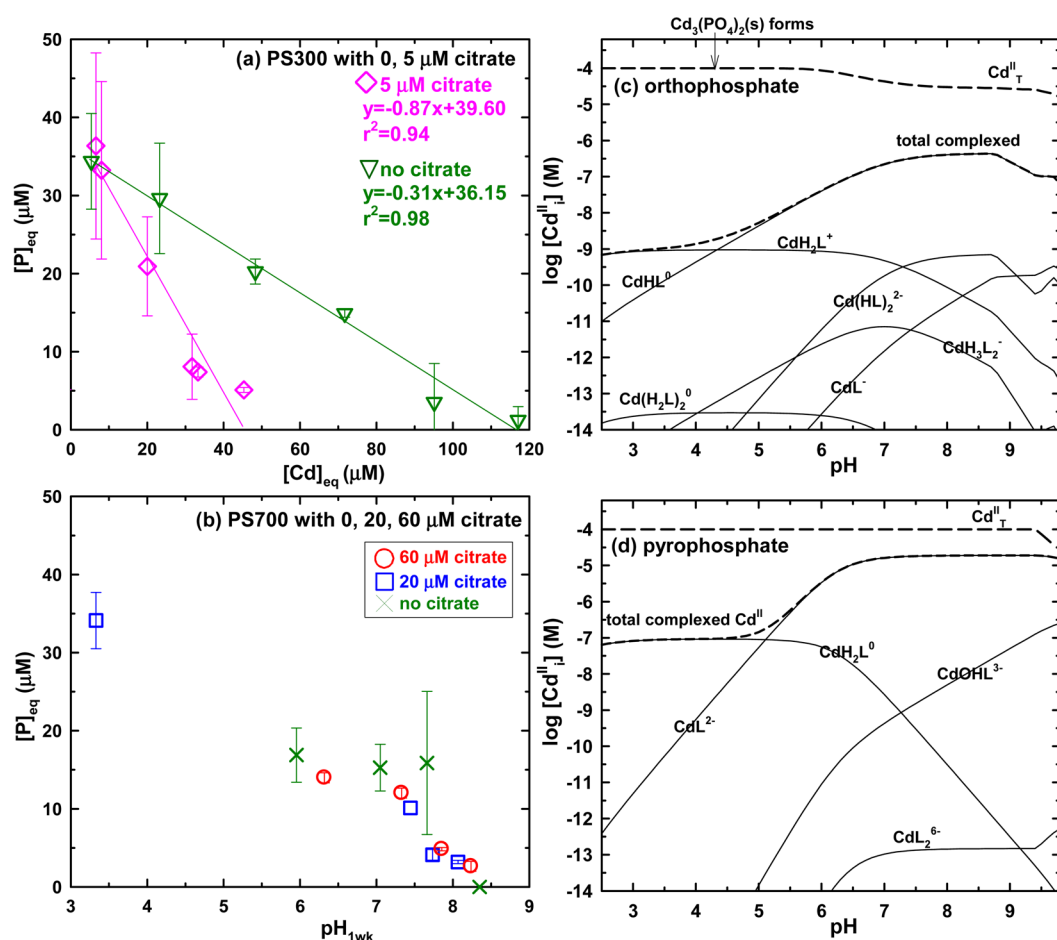


**Figure 5.** Equilibrium dissolved P concentration as a function of (a) Cd concentration for PS300 with 0 and 5  $\mu\text{M}$  citrate and (b)  $\text{pH}_{1wk}$  for PS700 with 0, 20, and 60  $\mu\text{M}$  citrate. Cd (100  $\mu\text{M}$  TOTCd, 10 mM NaCl) speciation with (c) 20  $\mu\text{M}$  orthophosphate and  $\text{Cd}_3(\text{PO}_4)_2(\text{s})$  as the solubility-limiting phase and (d) 20  $\mu\text{M}$  pyrophosphate and  $\text{Cd}(\text{OH})_2(\text{s}, \text{amorphous})$ .

shows the following trend in TOC at equilibrium: PS300 > PS700 (native pH) > PS700 (pH 6) > PS500. TOC did not show a clear trend with initial  $\text{Cd}^{II}$  concentration,  $\text{pH}_{48h}$ , or pyrolysis temperature (Figure 2c). However, Figure 2c indicates higher TOC at higher  $\text{pH}_{48h}$  (and  $\text{pH}_{1wk}$ ) for a given biochar (PS700). In addition, TOC of lower temperature biochar (PS300) was higher, as observed previously.<sup>9</sup>

**Influence of Citrate Concentration.** Citrate, a naturally occurring ligand with known stability constants,<sup>3</sup> was employed to investigate the influence of surface-bound and dissolved organic carbon on  $\text{Cd}^{II}$  sorption. Figure 3a presents sorbed  $\text{Cd}^{II}$  as a function of pyrolysis temperature in the presence of 5, 10, and 20  $\mu\text{M}$  citric acid. Biochars were pre-equilibrated with citric acid for 48 h before adding  $\text{Cd}^{II}$  (initial conditions: 100  $\mu\text{M}$   $\text{Cd}^{II}$  and 10  $\text{g L}^{-1}$  biochar at native pH). For PS700, 0–20  $\mu\text{M}$  citric acid did not influence  $\text{Cd}^{II}$  sorption (Figures 2a, 3a). As shown in Figure 3a, the presence of 5  $\mu\text{M}$  citric acid enhanced  $\text{Cd}^{II}$  sorption on lower temperature biochars to the degree of PS700. At 10–20  $\mu\text{M}$  citric acid,  $\text{Cd}^{II}$  sorption on 300–500  $^{\circ}\text{C}$  biochars decreased. For PS600,  $\text{Cd}^{II}$  sorption was similar for 5–10  $\mu\text{M}$  citric acid and decreased at 20  $\mu\text{M}$  citric acid (crosses in Figure 3a). Reduced  $\text{Cd}^{II}$  sorption at higher citric acid concentration results from the solution-phase complexation of  $\text{Cd}^{II}$  by citric acid. Ligands often cause a sigmoidal isotherm of metal sorption with an inflection point caused by ligand adsorption overcoming complexation.<sup>27</sup>

The constant  $\text{pH}_{1wk}$  (horizontal line) of  $7.6 \pm 0.3$  was observed for all experiments in Figures 3a–3b, regardless of citrate concentration or biochar type. Sorbed citrate facilitates the pH buffering ability of biochar. The  $\text{pK}_a$  of sorbed carboxylate ligands are estimated to be several units higher than the dissolved state.<sup>28</sup> The  $\text{pK}_a$  shift arises from unusually strong H-bonding interactions between the solute and surface functional group of sorbent having a comparable  $\text{pK}_a$ .<sup>28</sup> In experiments without citrate (Figures 1b, 2b),  $\text{pH}_{1wk}$  scattered around 7.5. Sorbed citrate likely enhanced the pH buffering ability of biochar to cause a constant  $\text{pH}_{1wk}$  of  $7.6 \pm 0.3$  in Figure 3b. The slope of  $\text{pH}_{48h}$  against  $\text{pH}_0$  (Figure 3b) indicates the release of  $\text{OH}^-$  during pre-equilibration for 20  $\mu\text{M}$  citrate. In unbuffered biochar suspension, carboxylate anion first exchanges proton with water to release  $\text{OH}^-$ .<sup>19</sup> The resulting neutral species forms a H-bond with aromatic  $-\text{COO}^-$  ( $\text{PZC} \approx 4$ ) of biochar.<sup>19</sup>

Figure 3c shows additional  $\text{Cd}^{II}$  species formed in the presence of 20  $\mu\text{M}$  citrate (5:1 molar ratio of  $\text{Cd}^{II}$ :citrate). Concentrations of  $\text{OH}^-$  and  $\text{Cl}^-$  species remained the same as Figure 1d. Within the pH range of experiments ( $\text{pH}_{48h}$  in Figure 3b),  $\text{Cd}(\text{OH})_2(\text{s}, \text{amorphous})$  does not form, and  $\text{Cd}^{II}$ –citrate complexes comprised only a small fraction (0.4  $\mu\text{M}$  at pH 5 to 13  $\mu\text{M}$  at pH 9) of total dissolved concentration ( $\text{Cd}^{II}_T \approx 100 \mu\text{M}$ ). Therefore, exceptionally reactive  $\text{Cd}^{II}$ –citrate species (despite low concentration, eq 2) and/or the citrate

sorbed on biochar caused the dramatic enhancement of  $\text{Cd}^{\text{II}}$  sorption in Figure 3a (triangles).

The lowest temperature biochar (PS300) had the highest O:C (0.26) and surface acidity ( $1.6 \pm 0.3$  mequiv  $\text{g}^{-1}$ ; Table S2, Supporting Information) and is expected to be enriched with oxygen-containing surface functional groups.<sup>29</sup> Figure 4a shows  $\text{Cd}^{\text{II}}$  sorption isotherms on PS300 with and without 5  $\mu\text{M}$  citrate. A progressive increase in  $q_s$  was observed with an increasing  $\text{Cd}^{\text{II}}$ :citrate molar ratio (4:1 to 24:1 along the  $x$ -axis in Figure 4a). In Figure 4b (crosses), equilibrium TOC increased 4-fold from 0 to 5  $\mu\text{M}$  citrate. Significant departure from TOC of 5  $\mu\text{M}$  citrate (0.36 ppmC) suggests the release of high molecular weight (MW) DOC from biochar.

To examine the contribution of high MW DOC in Figure 4b, TOC of low MW model ligands (Figure 4d) and high MW IHSS humic substances (Figure 4e) were determined. TOC of citrate (circles in Figure 4d) agreed with the theoretical values based on the elemental composition (horizontal lines). Compared to model ligands and other humic substances, TOC of Elliott soil humic acid (ESHA; triangles in Figure 4e) was significantly higher than the theoretical value (corrected for moisture and ash; pink horizontal lines in Figure 4e). ESHA represents a humic acid at an advanced stage of humification<sup>2</sup> and contains higher fixed C and aromatic C than reference Suwannee River natural organic (SRNOM)<sup>29</sup> having higher aliphatic components.<sup>30</sup> The TOC increase by added 5  $\mu\text{M}$  citrate (Figure 4b) is comparable to 100  $\text{mg L}^{-1}$  SRNOM in Figure 4e. Biochar (especially 350–500 °C)<sup>9</sup> contains organic compounds of different MW and water solubility: low MW (<600 Da) DOC rich in aromatic –COOH and –OH,<sup>31</sup> sparingly soluble polycyclic aromatic hydrocarbons (PAHs),<sup>32</sup> humic and biopolymer analogues,<sup>33</sup> and various volatile compounds.<sup>34,35</sup> Higher equilibrium pH (Figure 4c) in the presence of 5  $\mu\text{M}$  citrate (Figure 4c) could enhance the dissolution of humic-like macromolecules from DOC-enriched 300 °C biochar.<sup>9</sup>

Because  $\text{Cd}^{\text{II}}$  is a soft Lewis acid, sulfur-donor ligands (thiols) of biochar's DOC<sup>36</sup> can form inner-sphere complexes. Stronger tetrahedral complexes were formed between  $\text{Cd}^{\text{II}}$  and S-donor ligands of natural organic matter (NOM) than O- and N-donor ligands.<sup>37</sup> However, citric acid does not contain S, and the dissolution of S-containing DOC (of PS300) will decrease  $\text{Cd}^{\text{II}}$  sorption. Therefore, the S-complexation mechanism was ruled out. Alternatively,  $\text{Cd}^{\text{II}}$  may compete with DOC on available surface sites. However,  $\text{Cd}^{\text{II}}$  did not inhibit sorption of 2,4,6-trichlorophenol on wheat ash and humic acids, while  $\text{Cu}^{\text{II}}$  and  $\text{Pb}^{\text{II}}$  did.<sup>38</sup>

**Influence of Phosphate Ligands.** Amorphous  $\text{Cd}(\text{OH})_2$  having the solubility product constant ( $\log K_{\text{SO}}$ ) of  $-14.35$ .<sup>3</sup> was used as the solubility-limiting phase in Figures 1d and 3c.  $\text{Cd}^{\text{II}}$  also forms phosphate and carbonate phases with  $\log K_{\text{SO}}$  ranging from  $-12$  for  $\text{CdCO}_3$ <sup>39</sup> and  $-32.60$  for  $\text{Cd}_3(\text{PO}_4)_2$ <sup>40</sup> to  $-49.66$  for  $\text{Cd}_5(\text{PO}_4)_3\text{Cl}$ .<sup>40</sup> For example, X-ray diffraction analysis showed the formation of  $\text{Cd}_3(\text{PO}_4)_2(\text{s})$  on P-rich manure biochar but not on plant biochar.<sup>22</sup> In order to understand the influence of phosphate ligand, Figure 5a compares equilibrium P and  $\text{Cd}^{\text{II}}$  concentrations for 0 and 5  $\mu\text{M}$  citrate experiments in Figures 4a–c. For PS300, regardless of citrate addition, equilibrium P concentration decreased as a function of  $\text{Cd}^{\text{II}}$  concentration (Figure 5a), suggesting the formation of solubility-limiting  $\text{Cd}^{\text{II}}$  phosphate phases.<sup>22</sup> For PS700, equilibrium  $\text{Cd}^{\text{II}}$  and P concentrations did not correlate with one another. Instead, P concentration decreased as a

function of equilibrium pH (Figure 5b). Figure 5b was constructed for 5, 10, and 20  $\mu\text{M}$  citrate additions and shows similar pH dependence in all cases. Pyrophosphate is expected to be the primary dissolved P species in lower temperature biochar (PS300); orthophosphate becomes dominant at higher temperatures (PS700).<sup>41</sup> Pyrophosphate has greater  $\text{Cd}^{\text{II}}$  stability constant than orthophosphate (Table S1, Supporting Information), and cadmium pyrophosphate formation<sup>42</sup> can lead to the trend in Figure 5a. The  $\text{Cd}^{\text{II}}$  speciation diagrams were constructed for orthophosphate (Figure 5c,  $\text{Cd}_3(\text{PO}_4)_2(\text{s})$  as the solubility-limiting phase) and pyrophosphate (Figure 5d,  $\text{Cd}(\text{OH})_2(\text{s}, \text{amorphous})$  as the solubility-limiting phase). The arrow in Figure 5c indicates that  $\text{Cd}_3(\text{PO}_4)_2(\text{s})$  starts to form under acidic conditions to stabilize  $\text{Cd}^{\text{II}}$ . The 1:1 complexes with  $\text{Cd}^{\text{II}}$  increases as a function of pH for both orthophosphate and pyrophosphate and can contribute to “reactive” species in eq 2.

In conclusion,  $\text{Cd}^{\text{II}}$  sorption on biochar (regardless of pyrolysis temperature) progressively increased as a function of pH (Figure 1a). The pH trend suggested that  $\text{CdOH}^+$  and other hydrolysis products were the “reactive”  $\text{Cd}^{\text{II}}$  species engaging in the surface interaction with biochar. The reaction was strongly ionic strength dependent; 100 mM NaCl significantly diminished  $\text{Cd}^{\text{II}}$  sorption on biochar. Citric acid (0–20  $\mu\text{M}$ ) did not influence  $\text{Cd}^{\text{II}}$  sorption on 700 °C biochar. In contrast, 5  $\mu\text{M}$  citric acid significantly enhanced  $\text{Cd}^{\text{II}}$  sorption on 300–600 °C biochars; higher citrate concentration diminished  $\text{Cd}^{\text{II}}$  sorption. Trace citrate ( $[\text{Cd}^{\text{II}}]:[\text{citrate}]$  molar ratios of 4–24) (i) buffered pH of biochar suspension near 7 and (ii) dramatically increased DOC, after the reaction with  $\text{Cd}^{\text{II}}$ . Equilibrium P concentration correlated with  $\text{Cd}^{\text{II}}$  concentration for 300 °C (but not 700 °C) biochar.

There are several potential mechanisms for the enhanced  $\text{Cd}^{\text{II}}$  sorption and DOC release by a small amount of carboxylate ligand ( $[\text{Cd}^{\text{II}}]:[\text{citrate}]$  molar ratios of 4–24, Figure 4a). Sorbed multidentate ligand citrate can serve as a new sorption site for  $\text{Cd}^{\text{II}}$  and buffer pH near 7 (horizontal line in Figure 3b and crosses in Figure 4c). At higher (10–20  $\mu\text{M}$ ) citrate concentration, solution-phase  $\text{Cd}^{\text{II}}$  complexation out-competed the surface interaction involving sorbed citrate. In Figures 3–4, these effects of citrate concentration were observed for 300–500 °C biochars but not for PS700. The molar O:C ratio of biochar progressively decreases with the pyrolysis temperature (Table S2, Supporting Information), and PS700 is expected to contain the lowest –COOH and –OH functionalities. As a result, the  $[\text{Cd}^{\text{II}}]:[\text{citrate}]$  ratio (as low as 1) did not influence the ability of PS700 to sorb  $\text{Cd}^{\text{II}}$  at native pH. Citrate and related polydentate ligands have been used to produce chemically activated carbons.<sup>43</sup>  $\text{Cu}^{\text{II}}$  sorption was enhanced on a commercial-activated carbon prepared by soaking in concentrated citrate solution (1 M for 30 min and then washed and dried).<sup>43</sup> Sorption of citric acid on carbonaceous materials is expected to depend on the PZC<sup>44</sup> as well as  $\text{pK}_a$  of citric acid<sup>3</sup> that will influence the strength of H-bonding interactions.<sup>19</sup>

## ■ ASSOCIATED CONTENT

### Supporting Information

Proximate and ultimate analyses, total acidity measurement procedure and results, stability constants of  $\text{Cd}^{\text{II}}$  complexes, and pH immediately after  $\text{Cd}^{\text{II}}$  addition. This material is available free of charge via the Internet at <http://pubs.acs.org>.

## AUTHOR INFORMATION

## Corresponding Author

\*Fax: (504) 286-4367. Phone: (504) 286-4356. E-mail: sophie.uchimiya@ars.usda.gov.

## Notes

Mention of trade names or commercial products in this publication is solely for the purpose of providing specific information and does not imply recommendation or endorsement by the U.S. Department of Agriculture. USDA is an equal opportunity provider and employer.

The author declares no competing financial interest.

## REFERENCES

- (1) Uchimiya, M.; Lima, I. M.; Klasson, K. T.; Chang, S.; Wartelle, L. H.; Rodgers, J. E. Immobilization of heavy metal ions ( $\text{Cu}^{\text{II}}$ ,  $\text{Cd}^{\text{II}}$ ,  $\text{Ni}^{\text{II}}$ ,  $\text{Pb}^{\text{II}}$ ) by broiler litter-derived biochars in water and soil. *J. Agric. Food Chem.* **2010**, *58*, 5538–5544.
- (2) Spósito, G. *The Chemistry of Soils*; Oxford University Press: New York, 1989.
- (3) Martell, A. E.; Smith, R. M.; Motekaitis, R. J. *Critically Selected Stability Constants of Metal Complexes Database*, Version 8.0; U.S. Department of Commerce, National Institute of Standards and Technology: Gaithersburg, MD, 2004.
- (4) Stumm, W. Reactivity at the mineral-water interface: Dissolution and inhibition. *Colloids Surf., A* **1997**, *120*, 143–166.
- (5) Wieland, E.; Wehrli, B.; Stumm, W. The coordination chemistry of weathering: III. A generalization on the dissolution rates of minerals. *Geochim. Cosmochim. Acta* **1988**, *52*, 1969–1981.
- (6) Trivedi, P.; Axe, L. Predicting divalent metal sorption to hydrous Al, Fe, and Mn oxides. *Environ. Sci. Technol.* **2001**, *35*, 1779–1784.
- (7) Nowack, B.; Schulz, R.; Robinson, B. H. Critical assessment of chelant-enhanced metal phytoextraction. *Environ. Sci. Technol.* **2006**, *40*, 5225–5232.
- (8) Coughlin, B. R.; Stone, A. T. Nonreversible adsorption of divalent metal ions ( $\text{Mn}^{\text{II}}$ ,  $\text{Co}^{\text{II}}$ ,  $\text{Ni}^{\text{II}}$ ,  $\text{Cu}^{\text{II}}$ , and  $\text{Pb}^{\text{II}}$ ) onto goethite: Effects of acidification,  $\text{Fe}^{\text{II}}$  addition, and picolinic acid addition. *Environ. Sci. Technol.* **1995**, *29*, 2445–2455.
- (9) Uchimiya, M.; Ohno, T.; He, Z. Pyrolysis temperature-dependent release of dissolved organic carbon from plant, manure, and biorefinery wastes. *J. Anal. Appl. Pyrol.* **2013**, *104*, 84–94.
- (10) Stumm, W.; Morgan, J. J. *Aquatic Chemistry*; Wiley-Interscience: New York, 1996.
- (11) ASTM D7582: *Standard Test Methods for Proximate Analysis of Coal and Coke by Macro Thermogravimetric Analysis*; American Society for Testing and Materials: West Conshohocken, PA, 2010.
- (12) Boehm, H. P. Chemical identification of surface groups. *Adv. Catal.* **1966**, *16*, 179–274.
- (13) U.S. EPA Method 200.7: *Trace Elements in Water, Solids, and Biosolids by Inductively Coupled Plasma-Mass Spectrometry*, Revision 5.0; EPA-821-R-01-010; U.S. Environmental Protection Agency, Office of Research and Development, Cincinnati, OH, 2001.
- (14) Papelis, C.; Hayes, K. F.; Lechkie, J. O. *HYDRAQL: A Program for the Computation of Chemical Equilibrium Composition of Aqueous Batch Systems*, Version 1.0; 1988.
- (15) Uchimiya, M.; Wartelle, L. H.; Klasson, K. T.; Fortier, C. A.; Lima, I. M. Influence of pyrolysis temperature on biochar property and function as a heavy metal sorbent in soil. *J. Agric. Food Chem.* **2011**, *59*, 2501–2510.
- (16) Shinogi, Y.; Kanri, Y. Pyrolysis of plant, animal and human waste: Physical and chemical characterization of the pyrolytic products. *Bioresour. Technol.* **2003**, *90*, 241–247.
- (17) Lützenkirchen, J. Ionic strength effects on cation sorption to oxides: Macroscopic observations and their significance in microscopic interpretation. *J. Colloid Interface Sci.* **1997**, *195*, 149–155.
- (18) Fang, Q.; Chen, B.; Lin, Y.; Guan, Y. Aromatic and hydrophobic surfaces of wood-derived biochar enhance perchlorate adsorption via hydrogen bonding to oxygen-containing organic groups. *Environ. Sci. Technol.* **2014**, *48*, 279–288.
- (19) Ni, J.; Pignatello, J. J.; Xing, B. Adsorption of aromatic carboxylate ions to black carbon (biochar) is accompanied by proton exchange with water. *Environ. Sci. Technol.* **2011**, *45*, 9240–9248.
- (20) Yuan, J. H.; Xu, R. K.; Zhang, H. The forms of alkalis in the biochar produced from crop residues at different temperatures. *Bioresour. Technol.* **2011**, *102*, 3488–3497.
- (21) Inyang, M.; Gao, B.; Yao, Y.; Xue, Y.; Zimmerman, A. R.; Pullammanappallil, P.; Cao, X. Removal of heavy metals from aqueous solution by biochars derived from anaerobically digested biomass. *Bioresour. Technol.* **2012**, *110*, 50–56.
- (22) Xu, X.; Cao, X.; Zhao, L. Comparison of rice husk- and dairy manure-derived biochars for simultaneously removing heavy metals from aqueous solutions: Role of mineral components in biochars. *Chemosphere* **2013**, *92*, 955–961.
- (23) Wu, H.; Yip, K.; Kong, Z.; Li, C. Z.; Liu, D.; Yu, Y.; Gao, X. Removal and recycling of inherent inorganic nutrient species in mallee biomass and derived biochars by water leaching. *Ind. Eng. Chem. Res.* **2011**, *50*, 12143–12151.
- (24) Cowan, C. E.; Zachara, J. M.; Resch, C. T. Cadmium adsorption on iron oxides in the presence of alkaline-earth elements. *Environ. Sci. Technol.* **1991**, *25*, 437–446.
- (25) Schiewer, S.; Volesky, B. Ionic strength and electrostatic effects in biosorption of divalent metal ions and protons. *Environ. Sci. Technol.* **1997**, *31*, 2478–2485.
- (26) Silber, A.; Levkovitch, I.; Graber, E. R. pH-dependent mineral release and surface properties of cornstarch biochar: Agronomic implications. *Environ. Sci. Technol.* **2010**, *44*, 9318–9323.
- (27) Limousin, G.; Gaudet, J. P.; Charlet, L.; Szecknecht, S.; Barthes, V.; Krimissa, M. Sorption isotherms: A review on physical bases, modeling and measurement. *Appl. Geochem.* **2007**, *22*, 249–275.
- (28) Li, X.; Pignatello, J. J.; Wang, Y.; Xing, B. New insight into adsorption mechanism of ionizable compounds on carbon nanotubes. *Environ. Sci. Technol.* **2013**, *47*, 8334–8341.
- (29) Uchimiya, M.; Bannon, D. I.; Wartelle, L. H. Retention of heavy metals by carboxyl functional groups of biochars in small arms range soil. *J. Agric. Food Chem.* **2012**, *60*, 1798–1809.
- (30) Rakshit, S.; Uchimiya, M.; Spósito, G. Iron(III) bioreduction in soil in the presence of added humic substances. *Soil Sci. Soc. Am. J.* **2009**, *73*, 65–71.
- (31) Jamieson, T.; Sager, E.; Guéguen, C. Characterization of biochar-derived dissolved organic matter using UV-visible absorption and excitation-emission fluorescence spectroscopies. *Chemosphere* **2014**, *103*, 197–204.
- (32) Hale, S. E.; Lehmann, J.; Rutherford, D.; Zimmerman, A. R.; Bachmann, R. T.; Shitumbanuma, V.; O'Toole, A.; Sundqvist, K. L.; Arp, H. P. H.; Cornelissen, G. Quantifying the total and bioavailable polycyclic aromatic hydrocarbons and dioxins in biochars. *Environ. Sci. Technol.* **2012**, *46*, 2830–2838.
- (33) Lin, Y.; Munroe, P.; Joseph, S.; Henderson, R.; Ziolkowski, A. Water extractable organic carbon in untreated and chemical treated biochars. *Chemosphere* **2012**, *87*, 151–157.
- (34) Spokas, K. A.; Novak, J. M.; Stewart, C. E.; Cantrell, K. B.; Uchimiya, M.; DuSaire, M. G.; Ro, K. S. Qualitative analysis of volatile organic compounds on biochar. *Chemosphere* **2011**, *85*, 869–882.
- (35) Graber, E. R.; Tsechansky, L.; Lew, B.; Cohen, E. Reducing capacity of water extracts of biochars and their solubilization of soil Mn and Fe. *Eur. J. Soil Sci.* **2014**, *65*, 162–172.
- (36) Smith, C. R.; Sleighter, R. L.; Hatcher, P. G.; Lee, J. W. Molecular characterization of inhibiting biochar water-extractable substances using electrospray ionization fourier transform ion cyclotron resonance mass spectrometry. *Environ. Sci. Technol.* **2013**, *47*, 13294–13302.
- (37) Karlsson, T.; Persson, P.; Skyllberg, U. Extended X-ray absorption fine structure spectroscopy evidence for the complexation of cadmium by reduced sulfur groups in natural organic matter. *Environ. Sci. Technol.* **2005**, *39*, 3048–3055.



(38) Wang, Y. S.; Shan, X. Q.; Feng, M. H.; Chen, G. C.; Pei, Z. G.; Wen, B.; Liu, T.; Xie, Y. N.; Owens, G. Effects of copper, lead, and cadmium on the sorption of 2,4,6-trichlorophenol onto and desorption from wheat ash and two commercial humic acids. *Environ. Sci. Technol.* **2009**, *43*, 5726–5731.

(39) Thakur, S. K.; Tomar, N. K.; Pandeya, S. B. Influence of phosphate on cadmium sorption by calcium carbonate. *Geoderma* **2006**, *130*, 240–249.

(40) Crannell, B. S.; Eighmy, T. T.; Krzanowski, J. E.; Eusden, J. D., Jr.; Shaw, E. L.; Francis, C. A. Heavy metal stabilization in municipal solid waste combustion bottom ash using soluble phosphate. *Waste Manage.* **2000**, *20*, 135–148.

(41) Uchimiya, M.; Hiradate, S. Pyrolysis temperature-dependent changes in dissolved phosphorus speciation of plant and manure biochars. *J. Agric. Food Chem.* **2014**, *62*, 1802–1809.

(42) Clever, H. L.; Derrick, M. E.; Johnson, S. A. The solubility of some sparingly soluble salts of zinc and cadmium in water and in aqueous electrolyte solutions. *J. Phys. Chem. Ref. Data* **1992**, *21*, 941–966.

(43) Chen, J. P.; Wu, S.; Chong, K. H. Surface modification of a granular activated carbon by citric acid for enhancement of copper adsorption. *Carbon* **2003**, *41*, 1979–1986.

(44) Sreejalekshmi, K. G.; Krishnan, K. A.; Anirudhan, T. S. Adsorption of Pb(II) and Pb(II)-citric acid on sawdust activated carbon: Kinetic and equilibrium isotherm studies. *J. Hazard. Mater.* **2009**, *161*, 1506–1513.